An automatic static test system for gas sensor array

Peng-jun Yao[1,2], Jing Wang[1,#], Hai-ying Du[1,3], Mei-ying Su[1] and Jin-qing Qi[1]

1 School of Electronic Science and Technology, Dalian University of Technology, Dalian 116023, PR China
2 School of Educational Technology, Shenyang Normal University, Shenyang 110034, PR China
3 Department of Electromechanical Engineering & Information, Dalian Nationalities University, Dalian 116600, PR China
Corresponding Author / E-mail: wangjing@dlut.edu.cn, TEL: +86-411-8470-8382, FAX: +86-411-8470-6706

KEYWORDS : auto, static test system, gas sensing properties, Visual Basic, sensor

In this paper, we built an auto static test system for gas sensor array. Gas sensors are composed of alumina tubes with a pair of gold electrodes, on which $La_{0.7}Sr_{0.3}FeO_3$ nanowires are coated as a sensing material. A PC is used to control the heating voltage for the gas sensor array, monitor and record the change of resistance of the sensor array by a conventional circuit. Placed in a 50 L chamber, the gas sensor array is connected to a PC through a data acquisition card with a USB interface. Two solenoid valves and an air pump are also controlled automatically to allow air inlet and air outlet to be switched on or off. An output power supply is used to provide the heating voltage for the sensor array and controlled by the PC. Programs are designed in Visual Basic environment in our system to real-time monitor the response value and response transient. The curves of response vs. working temperature and response vs. gas concentrations are also presented in this system.

Manuscript received: January XX, 2011 / Accepted: January XX, 2011

1. Introduction

Gas sensors have a wide application in the fields such as monitoring and control environmental air quality, detection of flammable or toxic gases and medical diagnosis [1-3]. Metal oxide semiconductors are widely investigated as gas sensing materials due to their low cost, fast response and recovery time, excellent stability, high response value and simplicity of their use [4, 5]. This in turn requires a reliable test system that is able to simulate the entire range of ambient conditions that the gas sensor is likely to encounter. A static test system is often used in the gas sensing experiments because of low cost, flexibility and the similarity to application conditions [6-10].

Up to now, many kinds of auto dynamic test systems for gas sensing measurement have been reported [11-15], indicating that more attention have been attracted to the auto test system. The dynamic test method can achieve both accuracy and high dynamic range of adjustable concentrations, but the conditions in the chamber are different to practical application conditions. Moreover, the gas flow can affect the surface temperature of the gas sensors in dynamic test system, resulting to lower the operating temperature.

In this report, an automatic static test system for sensor array were presented, which employed a data acquisition card (USB 7360) with an USB interface and a power supply (Agilent E3631A) with a RS232 interface. Programs were designed in Visual Basic environment. A gas sensor array with $La_{0.7}Sr_{0.3}FeO_3$ nanowires as sensing materials was measured by using this system, showing this automatic test system to be practicable.

2. Experimental

2.1 Fabrication of gas sensor

$La_{0.7}Sr_{0.3}FeO_3$ nanowires sensing material was prepared by a hydrothermal method. In a typical synthesis process, 0.73 g cetyltrimethylammonium bromide (CTAB) was dissolved in 15 ml deionized water under continuous stirring until a homogeneous solution was obtained. The calculated amount of $La(NO_3)_3 \cdot 6H_2O$, $Sr(NO_3)_2$ and $Fe(NO_3)_3 \cdot 9H_2O$ were mixed with 10 ml deionized water. Subsequently, the nitrate aqueous solution was added into CTAB solution. After 30 min stirring, 15 ml $NH_3 \cdot H_2O$ (25% wt solution) was added dropwise into the mixed solution with vigorous stirring for 30 min. The mixture was then transferred to 50 ml Teflon lined stainless autoclave, sealed tightly and maintained at 180°C for 9 h, respectively. After that, the autoclave was allowed to cool down naturally. When the hydrothermal reaction was over, the precipitates were collected and washed several times with deionized water and ethanol. The washed precipitates were dried at 100°C for 24 h. The final products were obtained by annealing the as-synthesized product at 700°C for 6 h in air.

The as-annealed material was mixed and ground with deionized water in an agate mortar to form a paste. The paste was coated on an alumina tube (2 mm Ø × 4 mm) with a pair of gold electrodes to fabricate gas sensor [16]. Then the sensor was calcined at 600°C for 2

h. A Ni-Cr heating wire was inserted into the tube to use as a resistor to provide an operating temperature that was controlled by a heating voltage. The structure of the sensor is shown in Fig. 1. Lastly, the sensor was aged with an operating temperature 300°C in air for 240 h.

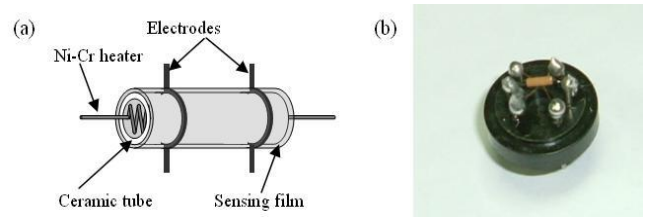

Fig. 1 (a) Schematic image of the sensor, (b) photograph of the $La_{0.7}Sr_{0.3}FeO_3$ gas sensor.

The morphology of the as-annealed sample was examined by scanning electron microscopy (SEM) on a Hitachi S-4800I (Japan) microscope.

2.2 System design

A schematic diagram of gas sensor array measurement set-up is displayed in Fig. 2. The measurement system is composed of three main parts:

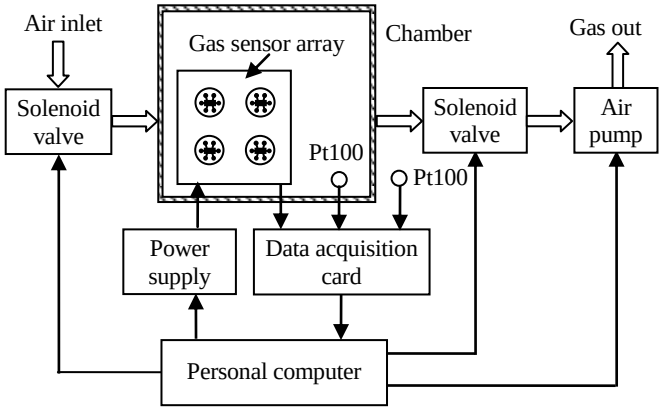

Fig. 2 Schematic diagram of the gas sensor array measurement set-up.

(1) Air flow part. This part includes two solenoid valves, a 50 L polytetrafluoroethene (PTFE) testing chamber (shown in Fig. 3) and air pump responsible for testing gas removed from the testing chamber. When the air pump works, fresh air is suctioned from the air inlet, passes the first solenoid valve and then reaches the chamber. The testing gas in the chamber will be taken away from the second solenoid valve. The fans in the testing chamber help to blow the testing gas out.

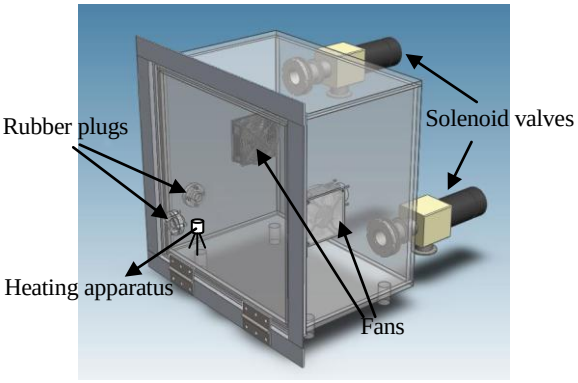

Fig. 3 Schematic diagram of testing chamber.

(2) Data acquisition part consists of an A/D USB data acquisition card (USB 7360, TZIC, China), with which two Pt100 probes and the gas sensor array are connected. Pt100 probes are used to monitor the temperature of inner chamber and ambient temperature, respectively.

(3) Control part controls the switches of two solenoid valve and air pump on or off. The heating voltage for the gas sensor provided by the power supply (Agilent E3631A) with a RS 232 interface is also included in this part. All the three parts are automatically controlled by a personal computer.

The gas sensor array was placed in the testing chamber. Each sensor's resistance was measured by using a conventional circuit displayed in Fig. 4. An external resistor was used to connect with the sensor in series at a circuit voltage of 5 V. The resistance of the gas sensor in target gas was calculated as the follows:

$$R_S = R_L \times (5\text{-}V_L)/V_L \quad (1)$$

where R_S and R_L are the resistances of the gas sensor and the reference resistor, respectively, and V_L is the measured voltage. The computer monitored and recoded the change of voltage signal V_L by an A/D data acquisition card.

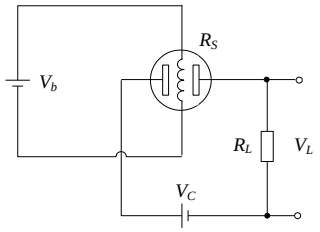

Fig. 4 Measurement circuit for gas sensor.

There are two ways to get required gas concentration in our systems:

(1) Injecting target gas. The target gas is injected into the chamber by a syringe through a rubber plug. Using this method, the volume (ml) of the injected gas can be calculated as

$$V=50000\times C/V_{bg} \quad (2)$$

where V is the volume of the injected gas, C is the concentration of the target gas (ppm), and V_{bg} is concentration of bottled gas (ppm).

(2) Injecting target liquid. The target liquid is injected into a heating apparatus (shown in Fig. 3) by a syringe through a rubber plug. The heating apparatus is made up of a heating wire and a quartz cup. At the heating temperature of 120°C provided by the heating apparatus, the target liquid will gasify quickly and mix with air in chamber helped by two fans. The volume (μl) of the injected target liquid (Q) [17] can be calculated as

$$Q=10^{-9}\times (V\times C\times M)/(22.4\times d\times p)\times (273+T_R)/(273+T_B) \quad (3)$$

where V is the volume of chamber (V=50000 ml in our system), M is the molecular weight of the target gas (g·mol^{-1}), C is the concentration of the target gas (ppm), d is the density of the target liquid (g·cm^{-3}), p is the purity of the liquid solution, T_R is the ambient temperature (°C) and T_B is the temperature (°C) of the inner chamber.

The measurement process of gas sensors is as follows:

1. The gas sensors are placed in the testing chamber and then the heating voltage is provided to the gas sensor array.

2. After two solenoid valves are switched on, the air pump begins to suction the air in the chamber for 5 min so as to keep the air in the chamber fresh.

3. Switch off the air pump, and then close the two solenoid valves.

4. Data acquisition card starts to collect the data of the gas sensor

array and Pt100 probes.

5. After the signals of the sensor array are stable, the calculated amount of target gas or target liquid was injected into the syringe in the chamber by a syringe through a rubber plug.

6. Record and monitor the variations of the signals until they reach equilibrium state.

7. Open the front door of the chamber to measure the recovery curves until the signals reach equilibrium state.

The sensor array is composed of four gas sensors in this system, but it can be extended the numbers of gas sensor to sixteen.

2.3 Programs design

The programs of the static test system were designed in Visual Basic environment. The programs can display voltage, resistance and response versus time of the gas sensor array. The response of the gas sensor is defined as $\beta=R_g/R_a$ [18, 19] or $\beta=R_a/R_g$ [20, 21] for $R_g > R_a$ or $R_a > R_g$, respectively, where R_g was the resistance of the gas sensor in target gas and R_a is the sensor resistance in pure air, respectively. For an *n*-type semiconductor, the sensor resistance decreases in the presence of reducing species and increases in the presence of oxidizing species. On the contrary, for a *p*-type semiconductor, the sensor resistance increases in the presence of reducing species and decreases in the presence of oxidizing species. The response time and recovery time were the time taken by the gas sensor to obtain 90% of the total resistance change in the adsorption and desorption processes, respectively.

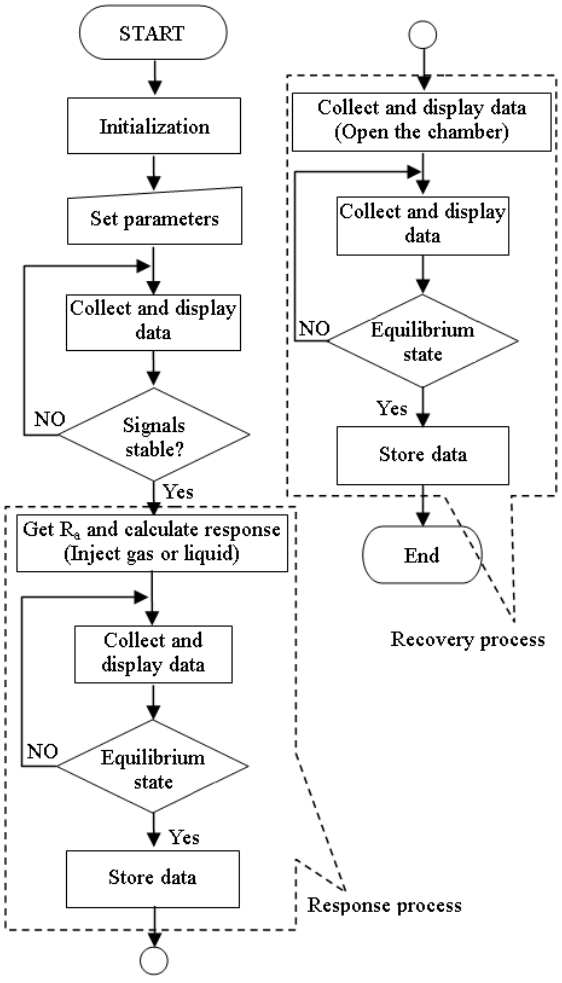

Fig. 5 Flowchart of the monitor and record programs

The flowcharts of the monitor and record programs are depicted in Fig. 5. The working process of the program is divided into three parts. The first part is responsible for initializing USB interface and RS232 interface, and setting parameters including the heating voltage, the resistances of the four reference resistors and the option of ratio R_g/R_a or R_a/R_g. The program to control the switch on and off of the two solenoid valves and air pump is included in the first part. The second part is response process. In this part, when the signals of resistances are stable, the stabilized value of the resistance is regarded as R_a before gas or liquid is injected. After the target gas or liquid is injected, the response process begins. The response process does not finish until the signals of the gas sensors are in equilibrium state. The last part is recovery process. When the signals are in equilibrium state, open the front door of the chamber. R_g goes back to R_a gradually as the gas in the chamber diffuses into the air. In these programs, the sampling interval is 1 s, and the signals of the gas sensor array are simultaneously collected and displayed.

3. Results and discussion

Fig. 6 depicts SEM images of $La_{0.7}Sr_{0.3}FeO_3$ nanowires. It is clearly seen that the sample is highly dominated by nanowires with lengths of several microns to tens of microns and diameters ranging from 100 to 150 nm (the largest length-to-diameter aspect ratio >100). Some thinner nanowires are also presented in Fig. 6.

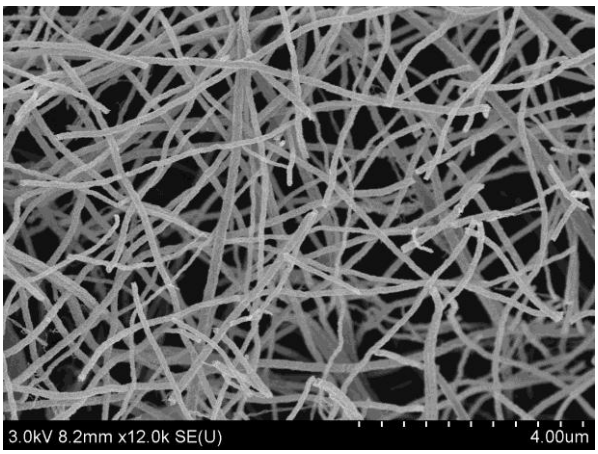

Fig. 6 SEM image of $La_{0.7}Sr_{0.3}FeO_3$ nanowires

Fig. 7 shows the software interface of the auto static test system. It shows the voltage curves of the $La_{0.7}Sr_{0.3}FeO_3$ nanowires gas sensor array in 0.1, 0.5 and 1 ppm HCHO, respectively. The four voltage curves corresponding to four gas sensors vary with HCHO concentration as time goes by. The operating temperatures of the sensors were 280°C. As could be seen in Fig. 7, the software interface of this system includes: (1) the setting resistances of the four reference resistors; (2) the option of the ratio R_g/R_a or R_a/R_g (R_g/R_a is chosen for $La_{0.7}Sr_{0.3}FeO_3$ gas sensors in HCHO); (3) the checkboxes of the measured gas sensors (all the four gas sensors are selected in this case); (4) the command buttons corresponding to data acquisition; (5) the temperature of inner chamber and ambient temperature. The software can provide voltage, resistance and response real-time curves and values.

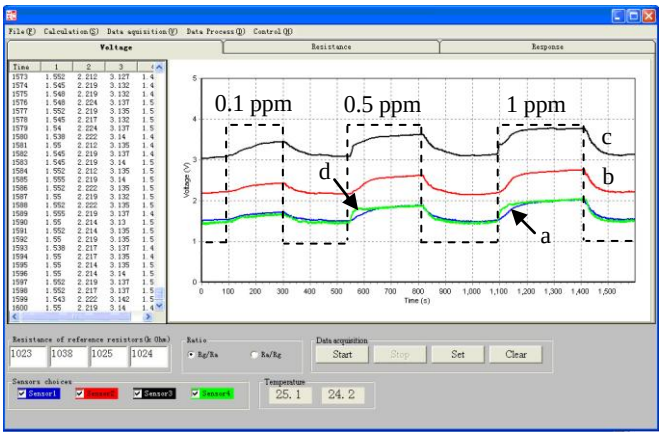

Fig. 7 Software interface of the auto static test system. Voltage curves of (a) sensor 1#, (b) sensor 2#, (c) sensor 3#, (d) sensor 4#.

The adsorption of the detected gas happens when semiconductor sensing material obtains some energy [22-25]. The energy of the gas sensors in this system is high temperature provided by a power supply. The operating temperature is one of the important parameters of a gas sensor, which has great effects on the response of the gas sensors. Fig. 8 shows the response of the gas sensor 2# to 20 ppm HCHO versus different operating temperature. The sensor displays maximum response to HCHO at 280°C. Below or above 280°C, the responses of the sensor to HCHO decrease. Thus, 280°C was selected as the optimum operating temperature of the gas sensors.

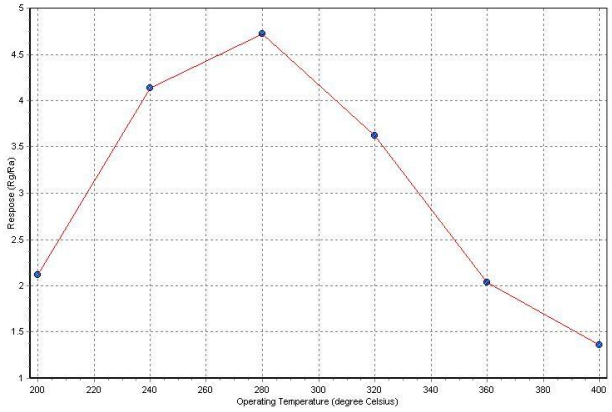

Fig. 8 Response of the sensor 2# to 20 ppm HCHO at different operating temperature.

The response of the sensor 2# versus HCHO concentration is depicted in Fig. 9. The response values increase from 1.32 to 8.21 as HCHO concentration varies from 0.1 to 100 ppm, respectively. The sensor can detect a concentration of formaldehyde as low as 0.1 ppm.

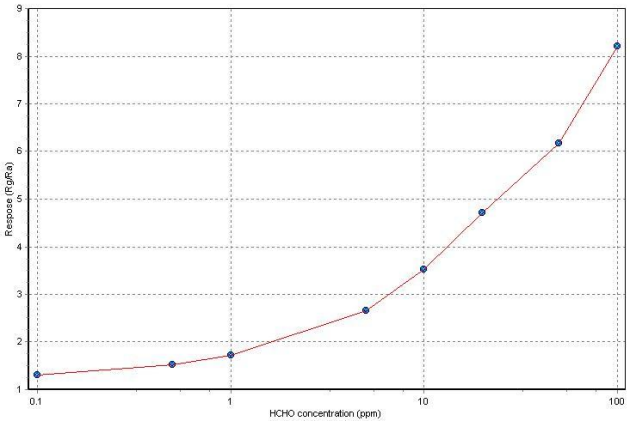

Fig. 9 Response of the sensor 2# vs. HCHO concentration.

The response transient of the sensor 2# to 20 ppm formaldehyde at operating temperature 280°C is shown in Fig. 10. The response and recovery times of the sensor to 20 ppm formaldehyde are 114 s and 52 s, respectively.

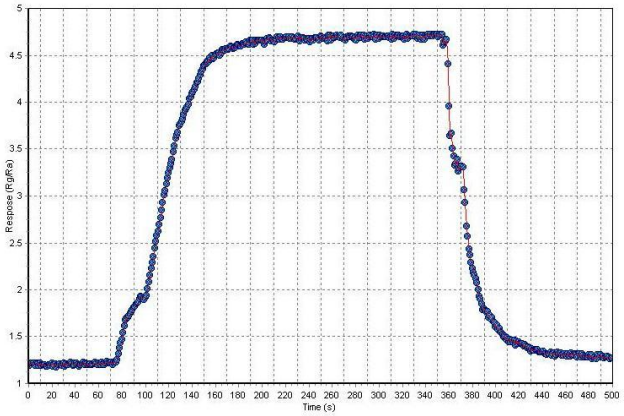

Fig. 10 Response transient of the sensor 2# to 20 ppm formaldehyde.

4. Conclusions

In this paper, an auto static test system for gas sensor array was developed, and the programs used in this system are designed in Visual Basic environment. The monitor, record and control the measurement processes were automatically realized by a PC. The measurement system consisted of three parts: air flow, data acquisition and control part. To get required gas concentration in our systems, two methods including injecting target gas and injecting target liquid were presented. The working process of the program was divided into initialization, response and recovery process. A sensor array with four gas sensors using $La_{0.7}Sr_{0.3}FeO_3$ nanowires as the sensing film was made and the voltage, resistance and response of the sensor were automatically measured by using this system. Furthermore, the response and recovery transient, the curves of the response vs. operating temperature, and the response vs. gas concentrations of the gas sensors were also presented in this system. These results reveal that the auto static test system can be practically used in measuring gas sensing properties. The sensors' numbers of the sensor array can be extended when needed in the future.

ACKNOWLEDGEMENT

The project is supported by the National Nature Science Foundati on of China (61001054).

REFERENCES

1. Wang, J., Zhang, P., Qi, J. Q. and Yao, P. J., "Silicon-based M icro-gas Sensors for Detecting Formaldehyde," Sens. Actuators B, Vol. 136, pp. 399-404, 2009.
2. Patila, D., Patilb, V. and Patila, P., "Highly Sensitive and Selective LPG Sensor based on α-Fe_2O_3 Nanorods," Sens. Actuators B, Vol. 152, pp. 299-306, 2011.

3. Yoo, J. and Wachsman, E. D., "NO_2/NO Response of Cr_2O_3- and SnO_2-based Potentiometric Sensors and Temperature-Actuators B, Vol. 123, pp. 915-921, 2007.
4. Yamazoe, N., Sakai, G. and Shimanoe, K., "Oxide Semiconductor Gas Sensors," Catal. Surv. Asia, Vol. 7, pp. 63-75, 2003.
5. Barsana, N., Kozieja, D. and Weimar, U., "Metal Oxide-based Gas Sensor Research: How to?," Sens. Actuators B, Vol. 121, pp. 18-35, 2007
6. Feng, Y. L., Wang, S. J., Feng, B., Wang, R., He, Y. and Zhang, T., "Development of an Auto Test System for Humidity Sensors," Sens. Actuators A, Vol. 152, pp. 104-109, 2009
7. Zhang, Y., Li, J. P., He, X.L., Gao, X. G. and Jia, J., "Deposition of Tin Oxide Nanofibers on a Microhotplate by a Controlled Electrospinning," Sens. Lett. , Vol. 6, No.6, pp. 956-960, 2008.
8. Zhang, Z. Y., Li, X. H., Wang, C. H., Wei, L. M., Liu, Y. C. and Shao, C. L., "ZnO Hollow Nanofibers: Fabrication from Facile Single Capillary Electrospinning and Applications in Gas Sensors," J. Phys. Chem. C, Vol. 113, pp.19397–19403, 2009.
9. Xu, J. Q., Chen, Y. P., L. Y. D. and Shen J. N., "Gas Sensing Properties of ZnO Nanorods Prepared by Hydrothermal Method," J. Mater. Sci., Vol. 40, No. 11, pp.2919-2921, 2005
10. Zhang, J. T., Liu, J. F., Peng, Q., Wang, X. and Li, Y. D., "Nearly Monodisperse Cu_2O and CuO Nanospheres: Preparation and Applications for Sensitive Gas Sensors," Chem. Mater., Vol. 18, No. 4, pp 867–871, 2006.
11. Demarne, V., Grisel, A., Sanjines, R. and Lévy, F., "Integrated Semiconductor Gas Sensors Evaluation with an Automatic Test System," Sens. Actuators B, Vol. 1, pp. 87-92, 1990.
12. Jerger, A., Kohler, H., Becker, F., Keller, H. B. and Seifert, R., "New Applications of Tin Oxide Gas Sensors: II. Intelligent Sensor System for Reliable Monitoring of Ammonia Leakages," Sens. Actuators B, Vol. 81, pp. 301-307, 2002.
13. Endres, H. E., Jander, H. D. and Göttler, W., "A Test System for Gas Sensors," Sens. Actuators B, Vol. 23, pp. 163-172, 1995.
14. Krebs, P., Grisel, A., "A Low Power Integrated Catalytic Gas Sensor," Sens. Actuators B, Vol. 13, pp. 155-158, 1993.
15. Nieuwenhuizen, M. S., and Harteveld, J. L. N., "An Automated SAW Gas Sensor Testing System," Sens. Actuators A, Vol. 44, pp. 219-229, 1994.
16. Wang, J., Liu, L., Cong, S. Y., Qi, J. Q. and Xu, B. K., "An Enrichment Method to Detect Low Concentration Formaldehyde," Sens. Actuators B, Vol. 134, pp.1010-1015, 2008.
17. Xu, L., Dong, B., Wang, Y., Bai, X., Liu, Q. and Song, H. W., "Electrospinning Preparation and Room Temperature Gas Sensing Properties of Porous In_2O_3 Nanotubes and Nanowires," Sens. Actuators B, Vol. 147, pp. 531-538, 2010.
18. Park, J. Y., Asokan, K., Choi, S. W. and Kim, S. S., "Growth Kinetics of Nanograins in SnO_2 Fibers and Size Dependent Sensing Properties," Sens. Actuators B, Vol. 152, pp. 254-260, 2011.
19. Feng, C. H., Ruan, S. P., Li, J. J., Zou, B., Luo, J. Y., Chen, W. Y., Dong, W. and Wu, F. Q., "Ethanol Sensing Properties of $LaCo_xFe_{1-x}O_3$ Nanoparticles: Effects of Calcination Temperature, Co-doping, and Carbon Nanotube-treatment," Sens. Actuators B, doi:10.1016/j.snb.2010.11.053
20. Hieu, N. V., Kim, H. R., B. K., Ju and Lee, J. H., "Enhanced Performance of SnO_2 Nanowires Ethanol Sensor by Functionalizing with La_2O_3," Sens. Actuators B, Vol. 133, pp. 228-234, 2008.
21. Choi, K. I., Kim, H. R. and Lee, J. H., "Enhanced CO Sensing Characteristics of Hierarchical and Hollow In_2O_3 Microspheres, Sens. Actuators B, Vol. 138, pp. 497-503, 2009.
22. Watson, J., Ihokura, K. and Coles, G. S. V., "The Tin Dioxide Gas sensor," Meas. Sci. Technol., Vol.4, pp.711-719, 1993.
23. Sun, Z. P., Liu, L., Zhang, L. and Jia, D. Z., "Rapid Synthesis of ZnO Nano-rods by One-step, Room-temperature, Solid-state Reaction and their Gas-sensing Properties," Nanotechnology, Vol. 17, pp. 2266–2270, 2006.
24. Zhang, J. T., Liu, J. F., Peng, Q., Wang, X. and Li, Y. D., "Nearly Monodisperse Cu_2O and CuO Nanospheres: Preparation and Applications for Sensitive Gas Sensors," Chem. Mater., Vol. 18, pp. 867-871, 2006.
25. Stankova, M., Vilanova, X., Llobet, E., Calderer, J., Bittencourt, C., Pireaux, J. J. and Correig, X., "Influence of the Annealing and Operating Temperatures on the Gas-sensing Properties of Rf Sputtered WO_3 Thin-film Sensors," Sens. Actuators B, Vol. 105, pp. 271–277, 2005.